

Structural, magnetic and thermal properties of $\text{CaMn}_{0.99}^{57}\text{Fe}_{0.01}\text{O}_{3-\delta}$

J. Przewoźnik*, J. Chmíst, L. Kolwicz-Chodak, Z. Tarnawski,
Cz. Kapusta, A. Kołodziejczyk

Department of Solid State Physics, Faculty of Physics and Applied Computer Science, AGH University of Science and Technology,
Av. Mickiewicza 30, 30-059 Cracow, Poland

Received 8 June 2006; received in revised form 29 August 2006; accepted 5 September 2006
Available online 30 January 2007

Abstract

The polycrystalline $\text{CaMn}_{0.99}^{57}\text{Fe}_{0.01}\text{O}_{3-\delta}$ compound was studied using powder X-ray diffraction, ^{57}Fe Mössbauer spectroscopy, ac susceptometry, dc magnetometry, specific heat and electrical resistivity measurements. X-ray diffraction measurements performed between 70 and 300 K show a thermal expansion anomaly at the Néel temperature. A weak ferromagnetic component and a spin-glass behaviour below Néel temperature are found in magnetic measurements. The Mössbauer spectroscopy measurements performed between 30 and 300 K provided the Néel temperature value of 118 K, the same as obtained from dc magnetisation and close to that derived from the specific heat (119 K). The temperature evolution of the Fe hyperfine field was analysed within a molecular field model and revealed equal strengths of the Fe–Mn and Mn–Mn exchange interactions in this compound.

© 2007 Elsevier B.V. All rights reserved.

PACS: 75.47.Lx; 75.40.Cx; 76.80.+y; 77.80.Bh; 72.80.–r; 65.40.De 75.30.Et

Keywords: Mössbauer spectroscopy; Magnetic measurements; X-ray diffraction; Oxide materials; Heat capacity

1. Introduction

The compound CaMnO_3 crystallises in the pseudo-cubic structure and has a simple G-type antiferromagnetic (AFM) order with T_N between 110 and 130 K [1]. It is an insulator with the theoretically predicted energy gap of 0.42 eV [2] but the activation energy (E_a) obtained from the electrical resistivity measurement amounts to 0.071 eV only [3], which is attributed to the thermal activation of charge carriers from impurity states associated with chemical defects. The compound shows a tendency to off-stoichiometry ($\text{CaMnO}_{3-\delta}$) due to the oxygen deficiency δ which is structurally accommodated by the presence of oxygen vacancies [4].

The main purpose of this work was to prepare the compound $\text{CaMn}_{0.99}^{57}\text{Fe}_{0.01}\text{O}_3$ lightly ^{57}Fe doped for Mössbauer measurements and to study its magnetic, structural and electronic properties as well as to compare the results with those obtained on mixed valence manganites [5,6].

2. Experimental results and their analysis

Polycrystalline sample of $\text{CaMn}_{0.99}^{57}\text{Fe}_{0.01}\text{O}_{3-\delta}$ was prepared by the standard solid-state reaction method by mixing stoichiometric quantities of CaCO_3 (99.95%), MnO_2 (99.9%) and $^{57}\text{Fe}_2\text{O}_3$. The mixture was heated at 1100 °C for 40 h in air and subsequently, at 1300 °C for 182 h, with several intermediate regrindings and final annealing at 1000 °C in air for 20 h. X-ray powder diffraction (XRD) measurements were performed on a Siemens D5000 diffractometer equipped with an Oxford Instruments gas flow cryostat using $\text{Cu K}\alpha$ radiation and a graphite monochromator. Powder XRD revealed no secondary phases. The refinement of the XRD patterns was carried out with the *Fullprof* program [7] assuming the GdFeO_3 -type perovskite structure and using the *Pbmm* space group. The fitted XRD pattern at 300 K is presented in Fig. 1 and the unit cell parameters are: $a = 5.2716(2)$ Å, $b = 5.2839(2)$ Å and $c = 7.4621(2)$ Å. Measurements performed between 70 and 300 K showed that the structure is preserved in this temperature range and the a , b and c parameters show a similar temperature behaviour. The temperature change of the unit cell volume V (inset of Fig. 1) shows an anomaly at 125 K reflected in different slopes of the polynomial fits (denoted by dashed lines) to the points below and above the anomaly, respectively.

The temperature dependence of the electrical resistivity R (not shown) was measured by the standard four-probe ac method. Above 90 K it follows the thermally activated behaviour $R = AT \exp(E_a/k_B T)$, with the activation energy $E_a = 0.144(1)$ eV. Magnetic characterization of the compound was performed with a conventional ac susceptometer at the excitation field of 0.5 Oe and the frequency of 188.9 Hz as well as with a VSM magnetometer. The dc magne-

* Corresponding author. Tel.: +48 12 617 36 07; fax: +48 12 634 12 47.
E-mail address: januszp@uci.agh.edu.pl (J. Przewoźnik).

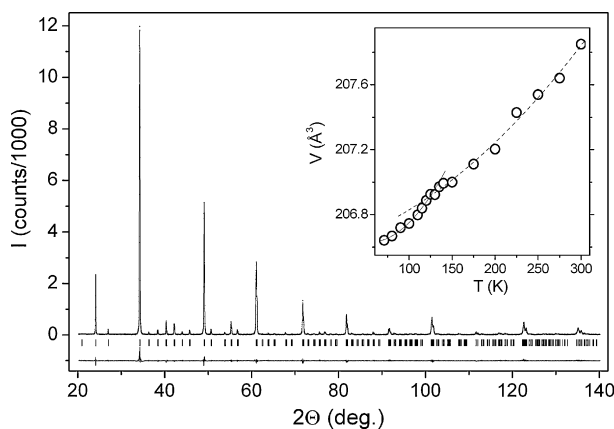


Fig. 1. XRD pattern of the $\text{CaMn}_{0.99}^{57}\text{Fe}_{0.01}\text{O}_{3-\delta}$ compound at 300 K. The inset shows temperature variation of the orthorhombic unit cell volume V (open symbols).

tization (M) was recorded during heating in the applied fields of 100 Oe after zero-field cooling (ZFC) and field cooling (FC) of the sample. Fig. 2a shows temperature dependences of the ZFC and FC magnetizations, which reveal a small ferromagnetic (FM) component and a spin-glass behaviour. Defining the T_N as the temperature corresponding to the minimum of dM/dT the value equal to 118 K was obtained. For a comparison, the temperature dependence of the real part of ac susceptibility (χ'_{ac}) is also plotted in Fig. 2a. It shows an unusually sharp and asymmetric cusp with maximum at the temperature 109 K, which is typical for spin-glass and is associated with the spin-glass freezing. The inset in Fig. 2a shows a hysteresis loop measured at 80 K. One should note a low values of M and a lack of saturation at the highest available magnetic field strength H .

The specific heat (c_p) measurement was carried out by the standard semi-adiabatic heat pulse method in the temperature range from 80 to 300 K on warming. Fig. 2b shows that the $c_p(T)$ curve exhibits a peak at T_N . In order to separate the lattice contribution and to estimate the magnetic contribution to

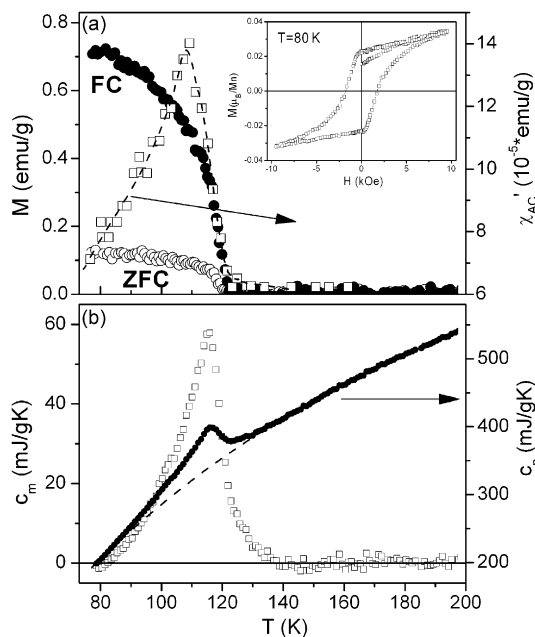


Fig. 2. (a) Zero-field (ZFC) and field cooled (FC) magnetization M and ac susceptibility χ'_{ac} as a function of temperature for $\text{CaMn}_{0.99}^{57}\text{Fe}_{0.01}\text{O}_{3-\delta}$. Dashed curve is a guide for eye. In the inset M vs. magnetic field H at 80 K is shown. (b) Temperature dependence of specific heat c_p and magnetic contributions to the specific heat c_m for $\text{CaMn}_{0.99}^{57}\text{Fe}_{0.01}\text{O}_{3-\delta}$. The meaning of dashed line is explained in text.

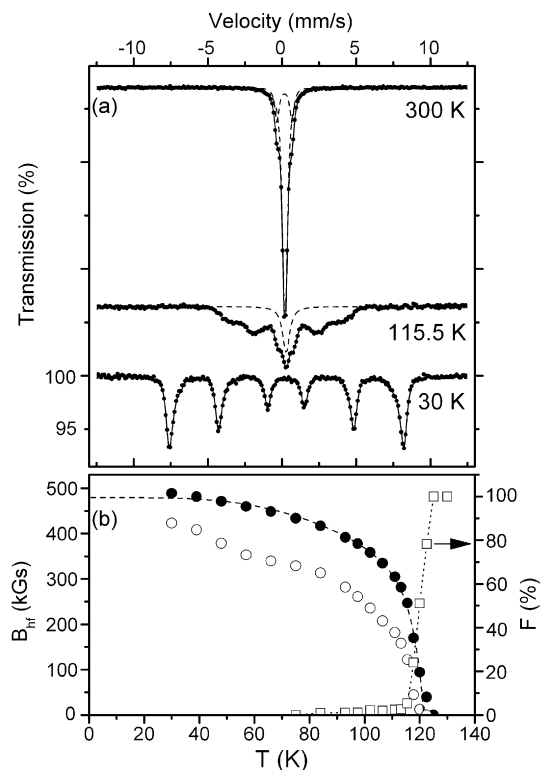


Fig. 3. (a) Temperature variation of the selected Mössbauer spectra. Solid lines denote the fits and dashed lines fitted contribution of paramagnetic phases (at 300 K two paramagnetic phases are shown). The base lines of the $T > 30$ K spectra are arbitrarily off-set. (b) Temperature dependence of mean hyperfine field B_{hf} for the majority (full circles) and minority (open circles) sites, and of the paramagnetic fraction F (open squares) obtained from Mössbauer spectra. The meaning of dashed line is explained in text. Dotted line is a guide for eye.

the specific heat (c_m) the points below 86 and above 145 K (far from the magnetic transition temperature) were fitted with a polynomial (denoted by dashed curve in Fig. 2b). The T_N value inferred from this measurement and defined as the temperature corresponding to the inflection point of the $c_m(T)$ amounts to 119 K and is in a good agreement with T_N obtained from magnetic measurements.

The ^{57}Fe Mössbauer spectroscopy (MS) study was performed in the transmission geometry using a constant acceleration type spectrometer employing a ^{57}Co in Rh source at 295 K. The sample studied was placed in a cryodyne refrigeration system (CTI-Cryogenics) and measurements were performed at the temperatures between 30 and 300 K. The representative Mössbauer spectra are shown in Fig. 3a. From room temperature down to 125 K the sample is paramagnetic (PM) and two quadrupole doublets can be fitted, as shown for the 300 K spectrum in Fig. 3a. At room temperature, the main doublet has the following hyperfine parameters: isomer shift $\text{IS} = 0.310(1)$ mm/s, quadrupole splitting $\text{QS} = 0.126(4)$ mm/s (IS values are given relative to $\alpha\text{-Fe}$ at 300 K) and line half-width $\Gamma = 0.158(3)$ mm/s. A second doublet with large $\text{QS} = 1.010(6)$ mm/s, smaller $\text{IS} = 0.278 \pm 0.002$ mm/s, $\Gamma = 0.160(5)$ mm/s and contribution 18.0(7)%, had to be included to obtain a good fit. The IS values indicate that the Fe ion is in high spin ($S = 5/2$, $3d^5$) $3+$ state. Nonzero QS has its origin in the orthorhombic distortion of the ideal perovskite structure and small value of QS for main doublet reflects the pseudo-cubic structure of a stoichiometric CaMnO_3 compound. The QS of the second doublet reflects a very distorted site, which is possibly due to vicinity of oxygen vacancy.

At 30 K a six-line spectrum for the AFM state is observed but some broadening and asymmetry of the lines is visible. The two sites model has been applied in the analysis of this spectrum. For the minority sites a contribution of 22(3)%, broader lines, but smaller effective hyperfine field ($\Delta B_{\text{hf}} = 30(3)$ kGs) and isomer shift ($\Delta \text{IS} = 0.06(2)$ mm/s) were found. Nearly zero values of the first order perturbation theory quadrupole shift parameter ε for both sites were found. To determine the temperature evolution of the hyperfine parameters and to model

the static distribution of the magnetic hyperfine fields (B_{hf}), the magnetically split spectra were fitted by an arbitrary number of magnetic sextets and PM doublets (up to 12), divided in two groups to maintain the two sites model. In all the fits common values of the IS, ε and Γ parameters were assumed for the sextets belonging to the same group but their contributions and B_{hf} parameters were treated as fitted parameters. Additionally, the total contributions for these two groups were constrained to 4:1 ratio and the largest B_{hf} of the minority group was checked to be smaller than all the B_{hf} in the majority group. A contribution of the PM phase was taken into account in the vicinity of T_{N} assuming the same values of QS and Γ parameters as in the spectrum measured above T_{N} at 130 K. The weighted mean values of B_{hf} (including PM component) for both sites and the contribution of the PM phase to the spectrum as a function of temperature are shown in Fig. 3b. The both B_{hf} curves show slightly different temperature behaviour. Defining the MS Néel temperature as the inflection point of the $B_{\text{hf}}(T)$ for the majority sites, the T_{N} value of 118 K was obtained. For $T \geq 115$ K rapidly growing contribution of the PM phase to the spectra is observed, which possibly results from local inhomogeneities caused by oxygen vacancies.

Temperature dependence of the experimental B_{hf} for the majority sites was fitted with the theoretical function (dashed line) based on the molecular field model [5,8]. It was assumed that in the $\text{Ca}(\text{Mn}_{0.99}^{57}\text{Fe}_{0.01})\text{O}_3$, the Fe^{3+} impurity ion with $S_{\text{Fe}} = 5/2$ is surrounded by 6 nearest-neighbours Mn^{4+} ions with $S_{\text{Mn}} = 1.5$ and its magnetic moment is antiferromagnetically coupled to those of adjacent Mn atoms. Assuming that the temperature dependence of the ^{57}Fe hyperfine field, which reflects the local $\langle S_{\text{Fe}} \rangle$, also follows the local manganese magnetisation, the following expression for $B_{\text{hf}}(T)$ was obtained:

$$B_{\text{hf}}(T) = B_{\text{hf}}(0)B_{S_{\text{Fe}}} \left[\frac{3S_{\text{Fe}}}{S_{\text{Mn}} + 1} \left(\frac{J_{\text{Fe-Mn}}}{J_{\text{Mn-Mn}}} \right) \left(\frac{T_{\text{N}}^*}{T} \right) \left(\frac{M_{\text{Mn}}(T)}{M_{\text{Mn}}(0)} \right) \right],$$

where $B_{S_{\text{Fe}}}$ is the Brillouin function, $J_{\text{Fe-Mn}}$, $J_{\text{Mn-Mn}}$ are exchange integrals and M_{Mn} denotes the manganese magnetization in the host lattice. Fitting this function to experimental points in Fig. 3b provided the value of the T_{N}^* equal to 121.4(2) K and the $J_{\text{Fe-Mn}}/J_{\text{Mn-Mn}}$ ratio equal to 1.07(2) was obtained. This reveals the same strength of the Fe–Mn and Mn–Mn superexchange interactions (SE) in this compound. The T_{N}^* can be compared to the magnetic ordering temperature obtained from the extrapolation of the maximal slope of the FC magnetization $M(T)$ curve to zero, which amounts to 122 K.

3. Discussion and conclusions

Our structural study of CaMnO_3 showed the pseudo-cubic perovskite structure with a good crystallinity but with larger unit cell volume ($\Delta V = 0.72 \text{ \AA}^3$) than expected for stoichiometric compound [3]. This indicates an oxygen deficiency of the compound. Larger T_{N} values, 130.8 K [9] and 125 K [3] reported for stoichiometric CaMnO_3 give further support for some oxygen deficiency δ in our compound. Electrical transport measurements on $\text{CaMnO}_{3-\delta}$ compounds with different δ parameter showed a decrease of activation energy E_{a} from 0.071 eV for $\delta = 0$ to about 0.022 eV for $\delta = 0.11$ [3]. This results stay in disagreement with a large E_{a} value (0.144(1) eV) obtained for our $\text{Ca}(\text{Mn}_{0.99}^{57}\text{Fe}_{0.01})\text{O}_{3-\delta}$ compound. The origin of this inconsistency is not clear. A small FM component observed in magnetization measurements, large disparity between FC and ZFC curves and a cusp in the ac susceptibility indicate a spin-glass behaviour. It can be related to the existence of oxygen vacancies which create local structural distortion and lead

to formation of Mn^{3+} sites. This can result in the occurrence of the $\text{Mn}^{3+}\text{--O--Mn}^{4+}$ double exchange (DE) FM interactions and a possible magnetic frustration. Therefore, it is natural to assign the observed minority sites with a large QS value in Mössbauer spectra to the Fe^{3+} ions occupying distorted sites with one oxygen vacancy in the octahedron (square pyramidal coordination). Assuming that oxygen vacancies are randomly distributed, one can correlate the fitted contribution of minority sites to the spectrum (18.0(7)%) with the oxygen deficiency parameter δ and estimate the stoichiometry of the compound as $\text{Ca}(\text{Mn}_{0.99}^{57}\text{Fe}_{0.01})\text{O}_{2.90}$.

Comparing the results with our earlier NMR and Mössbauer studies of mixed valence $\text{La}_{0.67}\text{Ca}_{0.33}\text{Mn}_{1-x}\text{M}_x\text{O}_3$ compounds (with $\text{M} = ^{57}\text{Fe}$, ^{119}Sn) [5,6] some clear differences should be noticed. The ^{55}Mn , ^{57}Fe and ^{119}Sn hyperfine fields remain finite at the Curie temperature determined from bulk magnetization measurements. This reveals a discontinuous character of the transition and the occurrence of the FM and PM phase segregation. In addition, the B_{hf} of Fe showed much different temperature behaviour than B_{hf} of host lattice Mn, which indicates a much different strength of the Fe–Mn SE and Mn–Mn DE interactions ($J_{\text{Fe-Mn}}/J_{\text{Mn-Mn}} \approx -0.5$). Also the T_{C}^* values derived from the mean field model were much higher than the corresponding T_{C} obtained from magnetization measurements. So the present study reveals a clear difference between the electronic and magnetic properties of the phase segregated FM mixed valence $\text{La}_{1-x}\text{Ca}_x\text{MnO}_3$ compounds and the insulating AFM parent $\text{CaMnO}_{3-\delta}$ compound.

Acknowledgement

Support from the Ministry of Science and Higher Education through the statutory funds for the Faculty of Physics and Applied Computer Sciences, AGH University of Science and Technology, Cracow, is acknowledged.

References

- [1] E.O. Wollan, W.C. Koehler, Phys. Rev. 100 (1955) 545–563.
- [2] W.E. Pickett, D.J. Singh, Phys. Rev. B 53 (1996) 1146–1160.
- [3] Z. Zeng, M. Greenblatt, M. Croft, Phys. Rev. B 59 (1999) 8784–8988.
- [4] E. Bakken, J. Boerio-Goates, T. Grande, B. Hovde, T. Norby, L. Rörmark, R. Stevens, S. Stølen, Solid State Ionics 176 (2005) 2261–2267.
- [5] J. Przewoźnik, Cz. Kapusta, J. Żukrowski, K. Krop, M. Sikora, D. Rybicki, D. Zajac, C.J. Oates, P.C. Riedi, Phys. Stat. Sol. (b) 243 (2006) 259–262.
- [6] J. Przewoźnik, J. Żukrowski, J. Chmista, E. Japa, A. Kołodziejczyk, K. Krop, K. Kellner, G. Gritzner, Nukleonika 49 (Suppl. 3) (2004) S37–S42.
- [7] J. Rodriguez-Carvajal, Physica B 192 (1993) 55–69.
- [8] V. Jaccarino, L.R. Walker, G.K. Wertheim, Phys. Rev. Lett. 13 (1964) 752–754.
- [9] J.J. Neumeier, D.H. Goodwin, J. Appl. Phys. 85 (1999) 5591–5593.